HHS Public Access

Author manuscript

Acta Biomater. Author manuscript; available in PMC 2022 October 26.

Published in final edited form as:

Acta Biomater. 2019 April 01; 88: 211–223. doi:10.1016/j.actbio.2019.02.037.

A genetically engineered Fc-binding amphiphilic polypeptide for congregating antibodies *in vivo*

Wen Liu[a], **Stephanie Wong-Noonan**[c], **Ngoc B. Pham**[a], **Isha Pradhan**[c], **Amy Spigelmyer**[a], **Riley Funk**[a], **Justin Nedzesky**[a], **Henry Cohen**[c], **Ellen S. Gawalt**[b,e], **Yong Fan**[c,d,*], **Wilson S. Meng**[a,e,*]

[a]Graduate School of Pharmaceutical Sciences, Duquesne University, Pittsburgh, PA 15282, USA

[b]Department of Chemistry and Biochemistry, Duquesne University, Pittsburgh, PA 15282, USA

[c]Institute of Cellular Therapeutics, Allegheny-Singer Research Institute, Pittsburgh, PA 15212, USA

[d]Department of Biological Sciences, Carnegie-Mellon University, Pittsburgh, PA 15213, USA

[e]McGowan Institute for Regenerative Medicine, University of Pittsburgh, PA 15213, USA

Abstract

We report herein an affinity-based hydrogel used in creating subcutaneous depots of antibodies *in vivo*. The biomaterials design centered on pG_EAK, a polypeptide we designed and expressed in *E. coli*. The sequence consists of a truncated protein G (pG) genetically fused with repeats of the amphiphilic sequence AEAEAKAK ("EAK"). Capture of IgG was demonstrated *in vitro* in gels prepared from admixing pG_EAK and EAK ("pG_EAK/EAK gel"). The binding affinities and kinetics of pG for IgG were recapitulated in the pG_EAK polypeptide. Injecting IgG antibodies formulated with pG_EAK/EAK gel into subcutaneous space resulted in retention of the antibodies at the site for at least six days, whereas only signal at background levels was detected in grafts injected with IgG formulated in saline or diffusion-driven gel. The local retention of IgG in pG_EAK/EAK gel was correlated with limited distribution of the antibody in liver, spleen and lymph nodes, in contrast to those injected with antibodies formulated in saline or non-Fc binding EAK gel. In addition, antibodies formulated with pG_EAK/EAK gel and injected in mouse footpads were found to retain at the site for 19 days. As a demonstration of potential bioengineering applications, thymic epithelial cells (TECs), the primary population of thymic stromal cells that are critical for the development of T-lymphocytes, were mixed with pG_EAK/EAK gel formulated with TEC-specific anti-EpCAM antibodies and injected subcutaneously into athymic nude mice. The injected TECs congregated into functional thymic units *in vivo*, supporting the development of both CD4+ and CD8+ T cells as well as Foxp3+ regulatory T cells in the mice. In conclusion, pG_EAK/EAK gel can be used to retain IgG locally *in vivo*, and can be tailored as scaffolds for controlling deposition of molecular and/or cellular therapeutics.

*Corresponding authors at: Duquesne University, Pittsburgh, PA 15282, USA (W. Meng). Allegheny Health Network, Pittsburgh, PA 15212, USA (Y. Fan). yongf@andrew.cmu.edu (Y. Fan), meng@duq.edu (W.S. Meng).

Appendix A. Supplementary data

Supplementary data to this article can be found online at https://doi.org/10.1016/j.actbio.2019.02.037.

Keywords

Hydrogels; Antibody; Self-assembling peptides; pG_EAK; EAK16-II; Multivalent assemblies; Biomolecular condensates; Thymic epithelial cells; Thymus organoid

1. Introduction

The rapid advances in antibody engineering have enabled the development of IgG and Fc-fusion molecules directed against diverse molecular targets, including cytokines and surface markers on immune cells [1]. While antibodies are typically formulated for systemic administration, strategies for localized delivery are being investigated for attaining high concentrations in targeted tissues while minimizing off-target toxicities [2–6]. Therapeutic antibodies and fusion proteins can also be administrated subcutaneously to modulate regional immune milieu in draining lymph nodes for treatment of chronic autoimmune ailments [7–9]. In addition, intratumoral injections are used for delivering antibodies aimed to modulate the tumor microenvironment in generating both local and systemic potent T cell responses in metastatic diseases [10].

Peptidic hydrogels are being investigated for creating depots of recombinant proteins *in vivo*. Among the systems studied are self-assembling peptides (SAP) by which gelation occurs *in situ* in response to local physiological cues [11,12]. The SAP EAK16-II (hereafter "EAK"), consisting of the sequence AEAEAKAKAEAEAKAK, which has an alternating pattern of charged and hydrophobic amino acids, self-assembles into cross-linking fibrils in ionic solutions [13]. However, IgG antibodies are rapidly released from the fibrillar matrices of EAK and the similar SAP RADA [14]. Inspired by systems of controlled release in polymeric gels modified with affinity ligands in heparin [15], divalent metal [16–18], and SH3 domain [19,20], we have engineered Fc-binding functions into EAK gels in formulating IgG for localized delivery [13,21,22]. The general strategy is to admix EAK with a second EAK-containing peptide fused with an affinity domain, such as His-tag [23,24] and dL5 [25,26]. The capture and release of IgG by these co-assemblies are governed in part by the equilibrium binding constant (K_D) of IgG interacting with protein A/G, which serves as a linker between the gel matrix and the antibody. Such coalescing systems are effective in extending the retention of a substantial fraction of IgG injected in skin allografts [27] and in subcutaneous tumors [28], from complete loss within one day to at least six days. One caveat with these systems is that the antibody is captured and released via two or three reversible interactions. While the designs provide high degrees of flexibility in the formulations, the complexities confound the understanding of the release kinetics of IgG from the gel matrices [25], thereby complicating dose optimization *in vivo*.

In the present paper, we report the characteristics of an Fc-binding SAP module, pG_EAK. This 25.3 kDa polypeptide consists of an N-terminal truncated protein G (pG) domain and a C-terminal EAK domain conjugated by a glycine-serine linker (Fig. 1a). The design leverages the ionic complementarity between the common AEAEAKAK-tract in assembling into stacked β-sheets. Solvent-exposed, Fc-binding domains of pG in the composites would interact with IgG constant regions (CH1-CH3) in a reversible manner. The premise was

that admixing pG_EAK with a molar excess of EAK would render β-fibrillar gels with multivalent Fc-binding sites [29].

Herein we present data showing that gels formed by admixing pG_EAK and EAK were used to control the release kinetics of IgG *in vivo*, as demonstrated by tracking the distribution of gel-formulated antibodies after local administration. In addition, we explored the feasibility of applying the pG_EAK platform to engineer functional tissue organoids for engraftment, by embedding and retaining tissue-specific cells in the composites with surface marker-targeting IgGs. To this end, thymic epithelial cells (TECs), the primary population of thymic stromal cells critical for T-cell development, were embedded in pG_EAK/EAK gel with an antibody against epithelial cell adhesion molecule (EpCAM), a surface marker for TECs. When injected into athymic nude mice, the TEC/pG_EAK composites effectively supported the development of functional T-cells, indicating that pG_EAK/EAK gel facilitated the formation of functional thymus organoids.

2. Methods and materials

2.1. Mice

All animal protocols were reviewed and approved by the Institutional Animal Care and Use Committees of Duquesne University and the Allegheny Singer Research Institute. Mice were housed in a certified or specific pathogen free environment. C57BL/6 and BALB/c mice were purchased from Hilltop lab animals (Scottdale, PA) and athymic B6.nude mice were purchased from the Jackson Laboratory (Bar Harbor, ME).

2.2. Peptides and reagents

The peptide AEAEAKAKAEAEAKAK, commonly referred to as EAK16-II and designated here as “EAK” was custom synthesized by EZBiolab (Carmel, IN) at greater than 95% purity with the N-terminus acetylated and C-terminus amidated. The sequence was confirmed by mass spectrometric analysis performed by the manufacturer. The peptide, received lyophilized, was reconstituted in sterile deionized water (18.2 MΩ at 25 °C) as needed and the solution was stored at −20 °C until use.

2.3. Expression of pG_EAK

A pET21 plasmid encoding pG_EAK was synthesized by engineering nucleotide sequence encoding both protein G [30] and EAK, together with 10X His GST HRV cleavage site into the plasmid. The predicted amino acid is shown in Figure S1. The plasmid was transformed into BL21(DE3) competent *E. coli.* (Invitrogen One shot®). The protein was purified using nickel resin and HRV protease, dialyzed and underwent endotoxin removal step.

2.4. Maldi-tof

The predicted molecular weight of the expressed fusion protein was confirmed using MALDI-TOF mass spectrometry. Purified pG_EAK was diluted 10 times to a final concentration of 5.46 μM, with 40 μL of this diluted solution combined with 10 μL of 0.5% TFA MilliQ-water. This protein solution was directly applied to target of Applied Biosystems Voyager DE-STR MALDI-TOF mass spectrometer.

2.5. Surface plasmon resonance

A Biacore T200 was used to determine the equilibrium and kinetic constants of pG_EAK and IgG antibodies. pG_EAK (0.92 mg/mL) was immobilized as ligand onto a CM5 chip using standard amine coupling chemistry. Four IgG and an Fc fusion protein were tested as analytes to flow over the ligand immobilized surface: mouse IgG1 (150 kDa, 3.3 μM stock concentration), Goat IgG (150 kDa, 6.7 μM stock concentration), rabbit IgG (150 kDa, 6.7 μM stock concentration) and human IgG (150 kDa, 6.7 μM stock concentration). The runs were conducted at 25 °C using a 20 mM phosphate buffer adjusted to pH 7.4 containing 2.7 mM KCl, 137 mM NaCl, 0.05% (v/v) and surfactant P20 was used as the running buffer. Different concentrations of the antibodies were used. Based on these captured ligand response values, theoretical R_{max} values were calculated. The flow rate of all analyte solutions was maintained at 50 μL/min. Association and dissociation times used for analytes were between 60 s and 1800 s, respectively. Sensorgrams from the overnight kinetics were evaluated using 1:1 steady state affinity or 1:1 kinetics model fitting.

2.6. Gel electrophoresis

Different amounts of EAK (10 μL, 20 μL, 40 μL or 80 μL, at 5 mg/mL) were added to 7.34 μL of pG_EAK (82.2 μM) to prepare mixtures of EAK and pG_EAK at different molar ratios (50:1, 100:1, 200:1 and 400:1) of the two components. Each mixture was q.s to a total volume of 500 μL and incubated overnight at 37 °C. The samples were centrifuged at 16,000 r.f.c. for 6 min with 5 μL of the supernatant analyzed using denaturing Novex SDS-PAGE gel electrophoresis (NuPAGE 4–12% Bis-Tris Electrophoresis system). For sample preparation, 5 μL of the supernatant was mixed with 5 μL of NuPAGE sample buffer and 10 μL of PBS. The mixtures were heated at 70 °C for 10 min before loading while 5 μL of the molecule maker was mixed with 10 μL of sample buffer and 25 μL of PBS without heating before loading. All samples were run at 200 V for 35 min in NuPAGE MES SDS running buffer. Fast silver staining procedure (SilverQuest™ staining kit) was used to visualize the protein bands. Gel images was captured using Kodak 440 image station and band intensities were quantified by Image J software. Percentage of pG_EAK incorporated into EAK coassemblies was calculated by subtracting the intensity of the protein band in samples containing EAK from the control sample with only pG_EAK in solution.

2.7. Enzymatic digestion of IgG

A chip-based SDS-PAGE was used to determine the extent to which pG_EAK interfered with the enzymatic degradation of polyclonal human immunoglobulins (hIgG) purified from serum (Sigma-Aldrich, St. Louis, MO). Trypsin was used as the model protease. Samples contained 0.135 mg/ml of hIgG, with or without pG_EAK, were centrifuged briefly (5 s at 10,000g) prior to addition of trypsin (Gibco; 0.15% in 1.33 mM EDTA). After one-hour incubation at 37 °C hour, the samples were analyzed using Agilent High Sensitivity Protein 250 chips under non-reducing condition and read using an Agilent Bioanalyzer 2100.

2.8. Congo red binding

A stock solution of 0.005% Congo red was prepared by diluting 30 μL of 0.1% of its aqueous solution using 570 μL of PBS. The absorbance spectra of Congo red were obtained

using a Tecan Infinite M1000 microplate reader after adding 40 μL of the stock solution to each of the samples containing 20 μL of EAK (5 mg/mL), 20.8 μL of pG_EAK (7.2 μM) or a mixture of the two (molar ratio of EAK: pG_EAK = 400:1). The samples were incubated for one hour before absorbance spectra measurement.

2.9. Viscosity measurement

Stock solutions of EAK and pG_EAK were prepared at 10 mg/ml in water and 9.26 μM in PBS respectively. Samples of EAK with or without pG_EAK were prepared in PBS and drew into positive displacement pipettes (RheoSense, Inc., San Ramon, CA). The ratio of EAK to pG_EAK was prepared at 400:1 and the final concentrations were 1.5 mg/mL and 2.3 μM, respectively. Measurements were conducted using the μVISC unit (RheoSense, Inc.) equipped with a temperature control module, which was set at 25 °C. Samples were subjected to different shear rates (1200–4000 s^{-1}) by changing the flow rate through the capillaries (depth = 50 um) in the sensor cartridge (HA01–01). Controls including pG_EAK alone and distilled water alone were measured at the same conditions.

2.10. Loading of IgG^{FITC} into pG_EAK/EAK gel

The binding of IgG to pG_EAK/EAK bioaffinity gel was measured by determining the loading of IgG on the hydrogel. Fluorescein (FITC) labeled IgG (Invitrogen) was used as the model IgG to provide the readout in the form of FITC fluorescence. 11.25 μg (75 pmol) of IgG^{FITC} was added to gel formed with 20 μL of 5 mg/ml EAK (60 nmol) and 24.5 μL of 6.16 μM pG_EAK (150 pmol) (molar ratio of EAK: pG_EAK = 400: 1). After being incubated for 15 min, the sample was brought up to 100 μL with PBS. The IgG^{FITC} loaded hydrogel was collected by centrifugation and washed with 1 ml of fresh PBS five times before re-suspended and transferred to a black 96 well plate for FITC fluorescence measurement. Control samples including IgG^{FITC} loaded in hydrogel made of only EAK, IgG^{FITC} mixed with only pG_EAK, or only IgG^{FITC} were also prepared by replacing EAK with water and pG_EAK with PBS.

2.11. Paper chromatography

The binding of IgG to pG_EAK/EAK gel was examined using a thin layer chromatography based on the trapping of IgG on the pathway of its migration driven by capillary action in chromatography papers (Whatman™ GE healthcare). Rabbit IgG^{800}s (NOVUS Biologicals, 1 mg/mL) were spotted horizontally near the edge; at about 3 cm above, PBS, EAK (5 μL of 5 mg/mL), or EAK and pG_EAK (5 μL of 5.46 μM) were spotted corresponding to each IgG spot vertically. The paper was then immersed in a reservoir filled with PBS, leaving a gap between the antibody spots and the solvent. The paper was removed from the reservoir once the solvent front moved to the top. The paper was allowed to dry and imaged using an Odyssey imager (Li-Cor, Inc., Lincoln, Nebraska) with the laser and camera set at low intensity (L2.0) and focus offset of 3.2 mm.

2.12. In vitro IgG release

The release kinetics of a fluorescein (FITC)-labeled IgG (Pierce goat anti-human IgG) from pG_EAK/EAK gel were determined by monitoring the cumulative fluorescence in release

media over 3 months. IgG-loaded gels were injected at the bottom of MicroSert (inner diameter = 4.15 mm, maximum volume = 500 μL) by instilling a mixture of EAK (60 nmol), pG_EAK (150 pmol) and IgG^{FITC} (75 pmol). The 55 μL mixture was incubated overnight at 37 °C before adding 400 μL of PBS containing 0.1% BSA, 0.024% NaN_3 as the release medium. The insert was placed in its receptacle vial and capped to prevent the medium evaporation. The vial was put under 37 °C for incubation. At various time points, 200 μL of the release medium were collected for measurement using plate reader (Perkin Elmer 1420 Multilabel Counter VICTOR™, excitation = 485 nm; emission = 535 nm). Aliquots of fresh release medium were added to restore the system to its initial volume. The apparent diffusivity (D_{app}) of IgG in pG_EAK/EAK gel was estimated by fitting the initial release to the non-steady state Fickian equation, relating M_t/M_∞ as a function of $t^{0.5}$.

2.13. Mouse in vivo retention studies in footpad, back and skin graft

Six to eight-week old female, certified-virus-free mice were quarantined for at least five days prior to use in experiments. Antibodies IgG^{800} (45 μg in 1 mg/mL goat anti-rabbit Dylight 800 4X PEG conjugate) by itself or the IgG^{800} displayed by pG_EAK/EAK gel were injected into the footpads (20 μL of 10 mg/mL EAK and 21.6 μL of 6.9 μM pG_EAK; n = 3) or back (80 μL of 10 mg/mL EAK and 82.4 μL of 14.556 μM pG_EAK; n = 4) of C57BL/6 mice. The infrared signal at the 800 nm channel in the footpad or on the mouse back was monitored at the local injection site using Li-Cor Pearl imager before and over 19 days (footpad) or 2 days (back) after the injection. Mice injected in the back were sacrificed at the end of the period and liver, spleen and lymph nodes were harvested for analysis using Odyssey imager at low intensity (L2.0) and the same focus offset (3.2 mm).

To demonstrate the stability of the affinity gel under inflammatory conditions, we used a murine allogeneic skin transplantation model (donor: BALB/c; recipient: C57BL/6) and tracked for 6 days after injection of an antibody. Mice between the ages of 8–12 weeks were randomized into three groups in the transplant experiments. The following formulations were used; IgG^{800} (11.24 μg in 1 mg/mL goat anti-rabbit Dylight 800 4X PEG conjugate), IgG^{800} displayed by EAK hydrogel (20 μL of 10 mg/mL EAK) or IgG^{800} displayed by pG_EAK/EAK gel (20 μL of 10 mg/mL EAK and 5.5 μL of 54.577 μM pG_EAK). The mixtures were injected subcutaneously underneath the skin graft (triplicates) two days after transplantation. Table 1 shows the formulations used in the *in vivo* experiments. The same threshold and resolution (170 μm) was used in all scanning, with the region of interest defined using an oval-shape at the contralateral flank as background. Fluorescence was quantified using the Impulse (2.0) software (Li-Cor, Inc.).

2.14. Isolation of thymic epithelial cells (TEC) and in vivo scaffolding

Thymi were harvested from 4 to 6 week old C57BL/6J mice. Thymic epithelial cells were isolated according to the procedure modified from previously described [31,32]. Briefly, thymus glands (n = 4) were needle dissected into half of the thymus lobe, and flushed with RPMI-1640 medium twice to remove released T cells. The tissues were then digested with Liberase solution [0.025 mg/mL Liberase™ (Roche Applied Science, Indianapolis), 0.2 mg/mL DNase I (Roche Applied Science), and 10 mM HEPES in RPMI-1640 (Life Technologies, Carlsbad, CA) at 37 °C in a gentleMACS™ Octo dissociator under program

37C_m_SDK_1. At the end of dissociation, the cell suspension was passed through a 40 μm filter and sorted using a microfluidic device according to the size. The enriched TEC fraction (fraction 2) was incubated with magnetic bead-conjugated anti-CD45 antibodies, and subjected to negative selection of CD45- thymic stromal cells (e.g. TECs and thymic fibroblasts) with MACS separation technology (Miltenyi Biotec, Auburn, CA). TECs were then labeled with Qtracker 800 by incubating the cells with 10 nM labeling solution made of mixture of Qtracker® component A and B from the labeling kit (molecular probes® by life technologies) for 1 h. Excess Qtracker 800 was removed by washing with complete RPMI-1640 medium twice. Isolated and stained TECs were mixed with anti-EpCAM IgG (11.25 μg, Biolegend), pG_EAK (4.34 μL of 69.2 μM) and EAK (20 μL of 10 mg/ml) to construct the thymus organoid and injected into the subcutaneous space in the back of the pinna of the right ears of syngeneic C57BL/6 mice (Triplicates). Qtracker 800 labeled free cells or TECs trapped in EAK gel were injected to the same site of different mice as the controls. The Qtracker 800 signal retained at the injection site was imaged on day 3 and day 7 using *in vivo* imager IVIS (Caliper).

2.15. Flow cytometry

Flow cytometric analysis was performed on the BD FACSCalibur flow cytometer (BD Biosciences, San Jose, CA) and analyzed with the CellQuest Pro software (BD Biosciences) or Flowjo. Splenocytes were treated with red blood cell lysis buffer (Sigma-Aldrich, St. Louis, MO). Before staining with antibodies of specific markers, single cells (isolated from either the spleens or the lymph nodes) were labeled with anti-CD16/32 IgGs for Fc-receptor blocking. The following antibodies were purchased from BD Biosciences: anti-CD16/32 (2.4G2), anti-CD4 (H129.9; RM4–5), anti-CD8 (53–6.7) anti-CD45 (30-F11), anti-CD3 (145–2C11), anti-EPCAM (g8.8), anti-γδ TCR (GL3), and anti-TCR β chain (H57–597). Staining buffer: phosphate buffered saline (PBS, calcium and magnesium free, Invitrogen) supplemented with 1% bovine serum albumin (BSA, Sigma-Aldrich) and 0.1% sodium azide (Sigma-Aldrich). Intracellular staining of the Foxp3 protein was performed with commercial kit purchased from eBiosciences (San Diego, CA), following manufacturer provided protocol.

2.16. T-cell proliferation assay

T-cells were isolated from the spleens and/or lymph nodes of B6.nude mice (n = 3) that were engrafted with the B6.TECs/pG_EAK/EAK thymus organoids (32-weeks post op). They were first labeled with carboxyfluorescein diacetate, succinimidyl ester (CFSE), and subsequently stimulated with allogeneic antigen presenting cells (harvested from the spleens of Balb/C mice). Proliferation of T-cells was evaluated by the dilution of CFSE intensities with FCM analyses, as previously described. Briefly, T-cells were suspended at a concentration of 10×10^6 cells/ml, mixed with equal volumes of diluted CFSE (5 μM), and incubated at 37 °C for 10 min. After extensive wash, 100 μL of CFSE-labeled in RMPI-10 (2.5×10^6 cells/ml) were mixed with 2.5×10^5 T-cell depleted, mitomycin C (Sigma) treated splenocytes harvested from Balb/C mice, and cultured for 7 days in wells of 96-well plates. Cells were stained with LIVE/DEAD fixable violet dyes (Life Technologies), followed by labeling with anti-CD4 and -CD8 antibodies (BD Biosciences) for FCM analyses. Unless specified otherwise, all the experiments were run in triplicate.

2.17. Statistical analysis

Statistical analysis was performed in GraphPad Prism 5.0. Data shown represent mean and standard mean error. In vitro pull-down assay data was analyzed with an unpaired *t*-test. *In vivo* fluorescence intensities in footpads were analyzed using Wilcox matched pairs test. Data from the *in vivo* retention of TECs in mouse ear pinna experiment were analyzed using one-way ANOVA and Tukey's multiple comparison test. Significance of T cell percentage and number differences in mice transplanted with TECs formulated in EAK or pG_EAK/EAK gel or no TEC control were determined using *t*-test. In all analysis of differences $p < 0.05$ was considered as statistically significant.

3. Results

The antibody–retentive function of pG_EAK/EAK gel was characterized *in vitro* and *in vivo*. The affinity-driven system hinges on the interactions between the pG domain and the constant region (Fc) of IgG antibodies. The polypeptide pG_EAK consists of a truncated protein G and EAK repeats separated by a glycine-serine linker (Fig. 1a). The protein G sequence was derived from *Streptococcus* sp. G418, encompassing the C1, C2, and C3 Fc-binding regions, devoid of the albumin-binding A and B domains in the native protein (pG_EAK nucleotide sequence is shown in supplemental data Fig. S1). The predicted molecular mass (M_r) of 25.3 kDa was confirmed using MALDI-TOF mass spectrometry (Supplemental data Fig. S2). First we examined the fibrillization potential of the pG_EAK polypeptide (Fig. 1b). Adding the polypeptide to a PBS solution of Congo red failed to shift the peak absorbance (peak = 486 nm), in contrast to samples containing EAK (peak = 510 nm). Thus, gelation of pG_EAK was enabled by admixing with excess EAK. It was determined that amalgamation of pG_EAK and EAK was most efficient at 400:1 M ratio of mixing, at which greater than 92% of the fusion polypeptide were removed from the supernatant, presumably incorporated into the fibrils (Fig. 1c). Except where stated otherwise, the experiments described herein were conducted using gels admixed at the 400:1 M ratio (EAK to pG_EAK).

The viscosity of the mixture at this ratio was tested using capillary rheometry, in which the pressure gradient across a microfluidic channel of an injected sample was registered [25,33]. Aqueous solutions containing EAK and/or pG_EAK were tested in a range of shear rates. Solutions dissolved with only pG_EAK exhibited baseline viscosity (Fig. 1d), which is consistent with the lack of fibril formation revealed in the Congo red experiment. At shear rate of 4,000 s^{-1}, the viscosity values of EAK, and pG_EAK mixed with EAK elevated above baseline, registering 2.3 ± 0.6 mPas and 2.5 ± 0.3 mPas, respectively, indicating that the materials could be injected using conventional 25 to 28-gauged needled syringes. At the low shear rate of 1200 s^{-1}, adding pG_EAK to EAK reduced the viscosity from 4.4 ± 0.3 mPas to 2.9 ± 0.9 mPas, suggesting interactions between the fusion peptide and EAK fibrils. Despite the low viscosity, pG_EAK/EAK gel adsorbed to a silica vessel and remained suspended for at least 24 h (Fig. 2d insert), indicating the mixture adopted a 3-dimensional structure.

3.1. Capture of IgG to pG_EAK polypeptide and in pG_EAK/EAK gel

The affinity and kinetic constants of pG_EAK for IgG were measured using SPR (Fig. 2a and Table 2). SPR chips were immobilized with pG_EAK (without EAK) and tested for interactions with mouse, goat, rabbit, human IgGs, and a mouse Fc fusion protein. The different clusters of lines represent binding curves tested at different concentrations of the antibody. Each cluster shows the steady state interaction of the antibody with the modified chip done in triplicate. Saturation of pG binding sites occurred by injecting 100 nM of the antibody. K_D was calculated based on curve fitting of data obtained at different antibody concentrations because equilibrium was achieved even in sub-saturation conditions. The combined profile is characteristic of a fast rate of association (k_a) and a slow dissociation (k_d).

The results indicate specific interactions of IgG with surface immobilized pG_EAK with K_D measured in the picomolar to nanomolar range, comparable to values reported in the literature for native protein G [34]. The differential affinities across the species reproduced the trend documented in the literature in that pG_EAK exhibited relatively weak affinities for mouse IgG1 and the Fc fusion protein [30]. In addition, the association and dissociation constants were found to be in the same magnitudes reported for the native proteins [35] (Table 2). These results show that the pG_EAK polypeptide recapitulated the IgG-binding properties of native protein G.

The extent to which pG_EAK/EAK gel displayed solvent-accessible Fc-binding sites was investigated in an *in vitro* pull-down assay (Fig. 2b). Close to 10-fold higher fluorescent intensity was observed in samples in which IgG^{FITC} admixed with pG_EAK and EAK, compared to samples containing the antibody mixed with only EAK. Mixing the antibody with pG_EAK but without EAK resulted in low amounts of fluorescent aggregates collected by centrifugation (10,000g). This result shows the weak fibrillization of the polypeptide without EAK. Association of IgG and pG_EAK/EAK gel was examined under a non-equilibrium condition using paper chromatography (Fig. 2c). Driven by capillary action, IgG^{800} accumulated at the point in the solvent pathway at which pG_EAK/EAK gel was spot. The crystal structures of protein G indicate a single α-helix stabilized by four β-strands [36], in which one of the strands interact with the CH1 domain of IgG [37]. We therefore postulated that such interactions might interfere with enzymatic degradation of IgG. To test this, human polyclonal IgG was digested with trypsin in the presence or absence of pG_EAK polypeptide. After one-hour incubation at 37 °C, the samples were analyzed in non-denaturing SDS-PAGE using the Agilent High Sensitivity Protein 250 chip (Fig. 3). In the absence of trypsin and pG_EAK, the antibody sample remained intact for the duration of the assay, as evidenced by the main peak at 150 kDa. In the presence of trypsin, multiple peaks with molecular mass below 20 kDa emerged with a significantly reduced 150 kDa peak. Addition of pG_EAK inhibited the degradation partially; the AUC of the 150 kDa peak was 5.7 and 6.7-fold higher compared to the same peak in samples without pG_EAK. Taken together, the data indicate that pG_EAK/EAK gel contains Fc-binding sites.

3.2. Kinetics of IgG release from pG_EAK/EAK gel in vitro

To gain insight into the microscopic properties of the affinity-driven process, release of antibodies from pG_EAK/EAK gel was monitored *in vitro* over a 12-week period (Fig. 4). The experiment was initiated by mixing IgG^{FITC} with pG_EAK and EAK in buffered saline in a cylindrical vessel of defined dimensions. In control experiments in which gels were made with only EAK, 85.2% ± 2.3% of the antibody loaded were released in the first 5 days. In contrast, a slow rate of release was observed with pG_EAK/EAK gel; by day 5, only 2.7% ± 0.5% of the IgG loaded were released. It was calculated that 82.7%± 0.02% of the IgG remained at the end of the 12-week period. The modified release was verified further in the apparent diffusivity (D_{app}) of IgG in pG_EAK/EAK gel. The initial phase of the release was fit to the non-steady state Fickian equation (Fig. 4; insert), which relate M_t/M_∞ as a function of $t^{0.5}$. D_{app} of IgG in pG_EAK/EAK gel was determined to be 5.6×10^{-5} m^2s^{-1}, three orders of magnitude lower than D_{app} of IgG embedded in EAK gel. The analysis shows that incorporating pG_EAK/EAK served to retain a large fraction of the IgG initially loaded in the matrix.

3.3. pG_EAK/EAK gel extends IgG localization in vivo

A pilot experiment showed that pG_EAK/EAK gel retained IgG in mouse footpads (Supplemental data Fig. S3). In a separate experiment, IgG^{800} injected in pG_EAK/EAK gel or in saline into mouse footpads were monitored for 19 days (Fig. 5). The signal declined sharply on day 1 in both groups, indicating diffusion of unbound antibodies from the injection site (Fig. 5a). From day 3 onward, the advantage of the gel was clear, with the retention of the antibody injected in pG_EAK/EAK gel sustained throughout (Fig. 5b). On day 19, the signal intensity in excised footpads (Fig. 5c) injected with IgG^{800} formulated with the gel was 5.3-fold higher than the antibody injected in saline (Fig. 5d). In another experiment, higher local fluorescence was observed in mice injected subcutaneously on the back with IgG^{800} mixed with pG_EAK/EAK gel, compared to mice injected with the antibody in saline (9-fold on day one and 12-fold on day 2; Fig. S4). Antibody distribution in the liver, spleen and lymph nodes was analyzed *ex vivo* on day 2 in euthanized mice. IgG^{800} delivered in saline appeared in the liver, spleen, and brachial, inguinal and sciatic lymph nodes, while the same antibody injected in pG_EAK/EAK gel was restricted to the immediate draining lymph nodes (Fig. S4c). These results indicate pG_EAK/EAK gel impeded the draining and distribution of IgG deposited at the subcutaneous injection site, thus confirming the retentive function of the affinity system.

Having established that the self-assembly and bioaffinity interactions took place *in vivo* in normal subcutaneous tissues, the capacity of pG_EAK/EAK gel to concentrate IgG in skin allografts was examined. The materials were injected into donor BALB/c ear skins grafted on the left side of recipient C57BL/6 mice, which invoked inflammation and cell-mediated immunity against the full-MHC mismatched tissues. IgG co-injected with pG_EAK/EAK gel into skin allografts were retained locally in mice for at least 6 days (Fig. 6a), concentrating in the center of the wound bed. Based on calculated AUC, approximately a 2-fold higher exposure was found in pG_EAK/EAK gel compared to the EAK and saline formulation groups (Fig. 6b). The higher graft retention also coincided with reduced

distribution to liver, lymph nodes, and spleen (Fig. 6c). These data show that pG_EAK/EAK gel can be deployed for displaying antibodies in inflammatory tissues.

3.4. T cell programming with TEC delivered with anti-EpCAM antibody-loaded pG_EAK/EAK gel

The antibody presenting and retaining properties of the pG_EAK/EAK gel prompted us to investigate whether the same platform can be used to regulate the organization of specific cells for engineering tissue organoids. Thymic epithelial cells (TECs) are the predominant population of thymic stromal cells that are essential for regulating key events in T cell lymphopoiesis, such as thymic homing of lymphocyte progenitors, T-cell lineage determination, recombination of T-cell receptor (TCR) genes and positive and negative selection of developing T-cells. Unlike epithelial cells underlining the skin and other tissues, the survival and function of TECs depend on the 3-dimensional (3D), extracellular matrix microenvironments of the thymus [38,39]. TECs grown as monolayer rapidly lose the expression of genes (e.g. MHC class II genes, Foxn1) essential for T-cell selection and succumb to apoptosis. To recreate the 3D microenvironment for TEC function and survival, TECs were admixed with pG_EAK/EAK gel formulated with antibodies against EpCAM, a surface marker for TECs, to form TEC organoids.

To examine the survival and local retention of TECs *in vivo*, CD45-EpCAM + TECs were isolated from C57BL/6 mice. To facilitate detection of the TECs in pG_EAK/EAK gel *in vivo*, the cells were stained with Qtracker 800 probes and the cells mixed with anti-EpCAM loaded pG_EAK/EAK gel was injected subcutaneously in the back of the pinna of the outer ears of syngeneic C57BL/6 mice. As shown in Fig. 7, Qdot-800 signal was detected at the injection site for as long as 7 days, at which time the signal from TECs injected in saline was declined to near background. The extent of retention of TECs injected in pG_EAK/EAK gel was significantly higher than that of cells injected with only EAK on day 7 (Fig. 7a). The decay profile of the labeled cells in pG_EAK/EAK gel parallels that of the antibody decay in that a shape decline was seen from time of injection to day 1, then sustaining until day 7 (Fig. 7b). These results suggest that the pG_EAK/EAK gel platform can prolong the survival of TECs *in vivo*.

To investigate the function of TECs embedded in pG_EAK/EAK gel to support T-lymphopoiesis *in vivo*, subcutaneous pinna injection was performed in syngeneic athymic B6.nude mice (designated as TECs/pG_EAK mice). The presence of CD45+ CD3+ T-cells in circulation was monitored in flow cytometric analyses of blood samples. At week 22, circulating T-cells in nude mice transplanted with TECs in pG_EAK/EAK gel increased significantly above those engrafted with TECs formulated with only EAK (designated as TECs/EAK mice; Fig. 8a). To further demonstrate the successful development of T-cells in TECs/pG_EAK mice engrafted with the TEC gel, T-cell composition in secondary lymphoid organs was examined at 32–36 weeks post-injection. Significantly higher numbers of T-cells were generated in TECs/pG_EAK mice, in comparison to TECs/EAK mice, as well as non-TEC-injected nude mouse controls (Fig. 8b and 8c). Development of both CD4+ T-helper cells and CD8+ cytotoxic T-lymphocytes are observed in TECs/pG_EAK mice (Fig. 8d). In addition, γδ-T cells, which play significant protective roles in mucosal immunity,

are also present (Fig. 8e). Moreover, CD4+ Foxp3+ T regulatory cells, the population of T-cells that are critical for maintaining immune self-tolerance in the periphery, were also generated, further suggesting that the TEC organoids formed in the pG_EAK/EAK platform can support the development of various subsets of T cells (Fig. 8f).

To examine the function of T cells derived from the thymus organoids, mixed leukocyte reaction (MLR) assays were performed to determine the cells' proliferating capacity upon TCR engagement. As shown in Fig. 8g ("B6.nude with thymus Tx"), T cells displayed significant proliferation against alloantigens, whereas only background levels of proliferation were detected upon supplement with syngeneic antigen presenting cells. The reactivity of T cells from wildtype B6 mice was shown as a control for T cell reactivity in immunocompetent hosts (Fig. 8g "B6"). These results suggest that TECs embedded pG_EAK/EAK gel injected subcutaneously can support the development of various subsets of T cells *in vivo*.

4. Discussion

The injectable gel of pG_EAK/EAK was designed around the concept of multivalent display of Fc-binding sites for antibody capture. The system employs a specific and reversible binding interaction thus can be used to control the release of IgG and/or Fc fusion proteins. Congregating multiple Fc-binding domains might increase the avidity of the binding. The data presented herein show that Fc-binding matrices are formed by mixing pG_EAK with the fibril-forming EAK. The immunoglobulin binding properties of native protein G are recapitulated in pG_EAK/EAK gel. The gel congregates antibodies *in vivo*, in normal subcutaneous tissue and in skin allografts. The system loaded with anti-EpCAM antibodies clusters epithelial cells subcutaneously, delivering TECs as functional thymic units in supporting T-cell development *in vivo*. These results support the notion that pG_EAK/EAK gel is an antibody delivery platform technology.

It is worth noting that the supramolecular assemblies of pG_EAK, EAK and IgG may be analogous to the biomolecular condensates recently discovered in eukaryotic cells [40]. Rosen and co-workers have observed a phenomenon of cytoplasmic phase-separation, in which proteins and nucleic acids concentrated in a small finite volume. In the extracellular space, pG_EAK/EAK gel resembles such condensates in steering the interactions of IgG with the local tissues. For macromolecules, lymphatic uptake is the main route of absorption from subcutaneous depots into the systemic circulation [41–43]. Preclinical studies indicate that diffusion of IgG through the extracellular matrix (ECM) is the ratelimiting step, given the relatively rapid transports from the lymph network to blood circulation [41]. In the ECM, IgG are degraded by proteolytic enzymes. This elimination pathway is compensated in part by endosomal recycling of IgG via neonatal Fc receptors (FcRn) expressed by local phagocytes, in which a fraction of the administered IgG is protected from proteases [42]. This is evidenced in studies using high doses of IgG (e.g. 100 mg/kg), which can saturate FcRn in local tissues, thereby increasing the fraction vulnerable to proteolysis. Mager and coworkers [42] have demonstrated this by monitoring subcutaneous-administered rituximab in rats, in which they observed a reduction of bioavailability from 31% to 18% corresponding to increasing the dose from 10 mg/kg to 40 mg/kg. We postulate that the

interaction between pG_EAK/EAK gel and IgG might inhibit the enzymatic digestion of the latter, thereby mimicking the protective effects of FcRn recycling in limiting the diffusion of IgG through the ECM.

The gap in durations between the *in vitro* release kinetics (Fig. 4) and the *in vivo* retention profiles of IgG (Figs. 5 and 6) in pG_EAK/EAK gel can be attributed to several factors. The ambient movements of the animals can disrupt the integrity of the localized soft gel, thereby increasing the rate of release. The lack of a strong buffering system in the subcutaneous space may allow the pH to drift, perturbing the affinities of pG for IgG in inflammatory tissues acidified by lactate [36]. The ionic strength *in vivo* may differ from the *in vitro* setting, as the former may not be fully hydrated. pG_EAK and EAK may be degraded through proteolysis in the extracellular space ; multiple cleavage sites are embedded within the pG_EAK sequence for peptidase-cleavage (based on PeptideCutter via ExPASy [44]; data not shown). The low viscosity of the gel is conducive to such cellular uptake. Eventually the materials would disintegrate after several weeks [45], most likely due to a combination of proteolytic degradation and macrophage phagocytosis.

Finally, our data suggest that pG_EAK/EAK gel can be applied as a biocompatible platform to facilitate the engineering and engraftment of functional tissue organoids *in vivo*. When injected subcutaneously in the pinna area in the back of the ear, TECs embedded in pG_EAK/EAK gel survived *in vivo* at least one week in the 3D fibrillar matrix environment. The thymus organoids formed by TECs and pG_EAK/EAK gel can promote the homing of common lymphocyte progenitors from the bone marrow and support the differentiation and selection of various subsets of T-cells to reestablish adaptive immune responses in athymic nude mice. Thus, pG_EAK/EAK gel can promote the formation of functional tissue organoids with isolated single cells *in situ* at the injection sites. Such an injectable platform is easy to administrate and retrieve, clearly advantageous to the traditional surgery-based procedure for solid organ/tissue transplantation. Moreover, the pG_EAK/EAK platform allows multivalent, multi-specific biologic presentations (e.g. VEGF and IL-10) that can be tailored to conditions of the injecting location (e.g. vascularization and immune tolerance induction, respectively), thereby facilitating the survival and function of the engraftments.

The design utilizes native binding affinities for displaying bioactive molecules, without the need for prior chemical modifications of the antibody being displayed or delivered. The rate of release can be controlled by varying the ratio of pG to antibody, thereby removing mesh size of the gel as a variable. Indeed, the current design was inspired by multivalent strategies used for enhancing bioactivities, through receptor clustering or interference with receptor mediated internalization [46–48]. The role of anti-EpCAM antibody in clustering TEC is attributed to blocking the negative regulator of E-Cadherin [49]. Expression of E-Cadherin drives aggregation of epithelial cells. Co-expression of EpCAM on the same cells disrupts the adhesive process by interfering the association of E-cadherin with the cytoskeleton via a decrease of a-catenin. While E-Cadherin conducts a strong adhesive force, EpCAM connects cells loosely. Thus by blocking EpCAM via the gel-tethered antibody in the extracellular space, E-Cadherin becomes the dominant adhesion molecule. The effect is likely due to keeping the antibody with the cells, blocking EpCAM continuously, rather than patterning. The dose was based on the assumption of bivalent interactions between pG_EAK and IgG

and the flexibility of modulating their ratio as a way to modify the release kinetics of the latter. The *in vitro* study ratio for pG_EAK to IgG was chosen as 2:1 to enhance the IgG interaction with pG embedded in the gel, minimizing the free antibody fraction trapped in the gel. Thus theoretically would result in a homogenous display of the antibodies [48].

In conclusion, the data presented herein support the notion of pG_EAK/EAK gel-enabled antibody deposition *in vivo*. The platform can be armed with multiple therapeutic antibodies, thereby enabling targeting distinct pathways simultaneously in pathogenic tissues and their draining lymph nodes. In combination therapies, the prolonged concentration of antibodies in draining lymph nodes could render synergistic impacts on multiple cellular and molecular entities driving pathogeneses. The specific utility of the system rests on the capability of controlling the fraction of free and bound antibody by varying the density of the Fc-binding domain in pG_EAK/EAK gel. This system of loco-regional drug delivery can reduce immune-related adverse events of many immune modulators currently approved for use in humans.

Supplementary Material

Refer to Web version on PubMed Central for supplementary material.

Acknowledgements

This work was supported in part by Department of Defense grant W81XWH1810644 (WSM), National Institutes of Health grants AI113000 (WSM), and AI123392 (YF). We thank Dr. Mat Saunders for designing the plasmid encoding pG_EAK, and Christina Bagia for the viscosity measurements. We acknowledge Logan Plath at Carnegie-Mellon University Center for Molecular Analysis for assistance in the mass spectrometric analysis. We are grateful to Dr. Aykut Uren at the Biacore Molecular Interaction Shared Resource for conducting the SPR measurements.

References

[1]. Hafeez U, Gan HK, Scott AM, Monoclonal antibodies as immunomodulatory therapy against cancer and autoimmune diseases, Curr. Opin. Pharmacol. 41 (2018)114–121. [PubMed: 29883853]

[2]. Bhattarai N, Gunn J, Zhang M, Chitosan-based hydrogels for controlled, localized drug delivery, Adv. Drug Deliv. Rev. 62 (1) (2010) 83–99. [PubMed: 19799949]

[3]. Friedrich EE, Azofiefa A, Fisch E, Washburn NR, Local Delivery of Antitumor Necrosis Factor-α Through Conjugation to Hyaluronic Acid: Dosing Strategies and Early Healing Effects in a Rat Burn Model, J. Burn Care Res. 36 (2) (2015) e90–e101. [PubMed: 25526179]

[4]. Sun LT, Bencherif SA, Gilbert TW, Lotze MT, Washburn NR, Design principles for cytokine-neutralizing gels: cross-linking effects, Acta biomaterialia 6 (12) (2010) 4708–4715. [PubMed: 20601239]

[5]. Friedrich EE, Washburn NR, Transport patterns of anti-TNF-alpha in burn wounds: therapeutic implications of hyaluronic acid conjugation, Biomaterials 114 (2017) 10–22. [PubMed: 27837681]

[6]. Korkmaz E, Friedrich EE, Ramadan MH, Erdos G, Mathers AR, Burak Ozdoganlar O, Washburn NR, Falo LD Jr., Therapeutic intradermal delivery of tumor necrosis factor-alpha antibodies using tip-loaded dissolvable microneedle arrays, Acta Biomater 24 (2015) 96–105. [PubMed: 26093066]

[7]. Balmert SC, Donahue C, Vu JR, Erdos G, Falo LD Jr., S.R. Little, In vivo induction of regulatory T cells promotes allergen tolerance and suppresses allergic contact dermatitis, J. Control Release 261 (2017) 223–233. [PubMed: 28694031]

[8]. Hotaling NA, Tang L, Irvine DJ, Babensee JE, Biomaterial Strategies for Immunomodulation, Annu. Rev. Biomed. Eng. (2015).

[9]. Hudalla GA, Modica JA, Tian YF, Rudra JS, Chong AS, Sun T, Mrksich M, Collier JH, A self-adjuvanting supramolecular vaccine carrying a folded protein antigen, Adv. Healthc. Mater. 2 (8) (2013) 1114–1119. [PubMed: 23436779]

[10]. Fransen MF, Arens R, Melief CJ, Local targets for immune therapy to cancer: tumor draining lymph nodes and tumor microenvironment, Int. J. Cancer 132 (9) (2013) 1971–1976. [PubMed: 22858832]

[11]. Wen Y, Collier JH, Supramolecular peptide vaccines: tuning adaptive immunity, Curr. Opin. Immunol. 35 (2015) 73–79. [PubMed: 26163376]

[12]. Hainline KM, Fries CN, Collier JH, Progress Toward the Clinical Translation of Bioinspired Peptide and Protein Assemblies, Adv. Healthc. Mater. 7 (5) (2018).

[13]. Zhang S, Holmes T, Lockshin C, Rich A, Spontaneous assembly of a self-complementary oligopeptide to form a stable macroscopic membrane, Proc. Natl Acad Sci U S A 90 (8) (1993) 3334–3338. [PubMed: 7682699]

[14]. Koutsopoulos S, Unsworth LD, Nagai Y, Zhang S, Controlled release of functional proteins through designer self-assembling peptide nanofiber hydrogel scaffold, Proc. Natl. Acad. Sci. USA 106 (12) (2009) 4623–4628. [PubMed: 19273853]

[15]. Wood MD, Hunter D, Mackinnon SE, Sakiyama-Elbert SE, Heparin-binding-affinity-based delivery systems releasing nerve growth factor enhance sciatic nerve regeneration, J. Biomater. Sci. Polym. Ed. 21 (6) (2010) 771–787. [PubMed: 20482984]

[16]. Lin CC, Metters AT, Bifunctional monolithic affinity hydrogels for dual-protein delivery, Biomacromolecules 9 (3) (2008) 789–795. [PubMed: 18257528]

[17]. Lin CC, Metters AT, Metal-chelating affinity hydrogels for sustained protein release, J. Biomed. Mater. Res. A 83 (4) (2007) 954–964. [PubMed: 17580324]

[18]. Lin CC, Metters AT, Enhanced protein delivery from photopolymerized hydrogels using a pseudospecific metal chelating ligand, Pharm. Res. 23 (3) (2006) 614–622. [PubMed: 16397740]

[19]. Pakulska MM, Vulic K, Shoichet MS, Affinity-based release of chondroitinase ABC from a modified methylcellulose hydrogel, J. Control. Release 171 (1) 11–16. [PubMed: 23831055]

[20]. Vulic K, Shoichet MS, Tunable growth factor delivery from injectable hydrogels for tissue engineering, J. Am. Chem. Soc. 134 (2) (2012) 882–885. [PubMed: 22201513]

[21]. Zhang S, Fabrication of novel biomaterials through molecular self-assembly, Nat. Biotechnol. 21 (10) (2003) 1171–1178. [PubMed: 14520402]

[22]. Keyes-Baig C, Duhamel J, Fung SY, Bezaire J, Chen P, Self-assembling peptide as a potential carrier of hydrophobic compounds, J. Am. Chem. Soc. 126 (24) (2004) 7522–7532. [PubMed: 15198599]

[23]. Condamine T, Gabrilovich DI, Molecular mechanisms regulating myeloid-derived suppressor cell differentiation and function, Trends Immunol. 32 (1) (2011)19–25. [PubMed: 21067974]

[24]. Zheng Y, Wen Y, George AM, Steinbach AM, Phillips BE, Giannoukakis N, Gawalt ES, Meng WS, A peptide-based material platform for displaying antibodies to engage T cells, Biomaterials 32 (1) (2011) 249–257. [PubMed: 20880580]

[25]. Liu W, Saunders MJ, Bagia C, Freeman EC,Fan Y, Gawalt ES, Waggoner AS, Meng WS, Local retention of antibodies in vivo with an injectable film embedded with a fluorogen-activating protein, J. Control. Release 230 (2016) 1–12. [PubMed: 27038493]

[26]. Saunders MJ, Liu W, Szent-Gyorgyi C, Wen Y, Drennen Z, Waggoner AS, Meng WS, Engineering fluorogen activating proteins into self-assembling materials, Bioconjug. Chem. 24 (5) (2013) 803–810. [PubMed: 23573960]

[27]. Wen Y, Liu W, Bagia C, Zhang S, Bai M, Janjic JM, Giannoukakis N, Gawalt ES, Meng WS, Antibody-functionalized peptidic membranes for neutralization of allogeneic skin antigen-presenting cells, Acta Biomater 10 (2014) 4759–4767. [PubMed: 25117952]

[28]. Wen Y, Kolonich HR, Kruszewski KM, Giannoukakis N, Gawalt ES, Meng WS, Retaining antibodies in tumors with a self-assembling injectable system, Mol. Pharm. 10 (3) (2013) 1035–1044. [PubMed: 23419203]

[29]. Gasiorowski JZ, Collier JH, Directed intermixing in multicomponent self-assembling biomaterials, Biomacromolecules 12 (10) (2011) 3549–3558. [PubMed: 21863894]

[30]. Guss B, Eliasson M, Olsson A, Uhlen M, Frej AK, Jornvall H, Flock JI, Lindberg M, Structure of the IgG-binding regions of streptococcal protein G, EMBO J. 5 (7) (1986) 1567–1575. [PubMed: 3017704]

[31]. Tajima A, Liu W, Pradhan I, Bertera S, Bagia C, Trucco M, Meng WS, Fan Y, Bioengineering mini functional thymic units with EAK16-II/EAKIIH6 self-assembling hydrogel, Clin. Immunol. (2015).

[32]. Tajima A, Liu W, Pradhan I, Bertera S, Lakomy RA, Rudert WA, Trucco M, Meng WS, Fan Y, Promoting 3-D Aggregation of FACS Purified Thymic Epithelial Cells with EAK16-II/EAKIIH6 Self-assembling Hydrogel, J. Visualized Exp. : JoVE 112 (2016).

[33]. Zarraga IE, Taing R, Zarzar J, Luoma J, Hsiung J, Patel A, Lim FJ, High shear rheology and anisotropy in concentrated solutions of monoclonal antibodies, J. Pharm. Sci. 102 (8) (2013) 2538–2549. [PubMed: 23873347]

[34]. Akerstrom B, Bjorck L, A physicochemical study of protein G, a molecule with unique immunoglobulin G-binding properties, J. Biol. Chem. 261 (22) (1986) 10240–10247. [PubMed: 3733709]

[35]. Saha K, Bender F, Gizeli E, Comparative study of IgG binding to proteins G and A: nonequilibrium kinetic and binding constant determination with the acoustic waveguide device, Anal. Chem. 75 (4) (2003) 835–842. [PubMed: 12622374]

[36]. Bryers JD, Giachelli CM, Ratner BD, Engineering biomaterials to integrate and heal: the biocompatibility paradigm shifts, Biotechnol. Bioeng. 109 (8) 1898–1911.

[37]. Gouda H, Shiraishi M, Takahashi H, Kato K, Torigoe H, Arata Y, Shimada I, NMR study of the interaction between the B domain of staphylococcal protein A and the Fc portion of immunoglobulin G, Biochemistry 37 (1) (1998) 129–136. [PubMed: 9425032]

[38]. Fan Y, Tajima A, Goh SK, Geng X, Gualtierotti G, Grupillo M, Coppola A, Bertera S, Rudert WA, Banerjee I, Bottino R, Trucco M, Bioengineering Thymus Organoids to Restore Thymic Function and Induce Donor-Specific Immune Tolerance to Allografts, Molecular therapy : the Journal of the American Society of Gene Therapy 23 (7) (2015) 1262–1277. [PubMed: 25903472]

[39]. Tajima A, Pradhan I, Trucco M, Fan Y, Restoration of Thymus Function with Bioengineered Thymus Organoids, Curr. Stem Cell Reports 2 (2) (2016) 128–139.

[40]. Banani SF, Lee HO, Hyman AA, Rosen MK, Biomolecular condensates: organizers of cellular biochemistry, Nat. Rev. Mol. Cell Biol. 18 (5) (2017) 285–298. [PubMed: 28225081]

[41]. Kagan L, Pharmacokinetic modeling of the subcutaneous absorption of therapeutic proteins, Drug metabolism and disposition: the biological fate of chemicals 42 (11) (2014) 1890–1905. [PubMed: 25122564]

[42]. Kagan L, Turner MR, Balu-Iyer SV, Mager DE, Subcutaneous absorption of monoclonal antibodies: role of dose, site of injection, and injection volume on rituximab pharmacokinetics in rats, Pharm. Res. 29 (2) (2012) 490–499. [PubMed: 21887597]

[43]. Dahlberg AM, Kaminskas LM, Smith A, Nicolazzo JA, Porter CJ, Bulitta JB, McIntosh MP, The lymphatic system plays a major role in the intravenous and subcutaneous pharmacokinetics of trastuzumab in rats, Mol. Pharm. 11 (2) 496–504. [PubMed: 24350780]

[44]. Wilkins MR, Gasteiger E, Bairoch A, Sanchez JC, Williams KL, Appel RD, Hochstrasser D, Protein identification and analysis tools in the ExPASy server, Methods in molecular biology (Clifton, N.J.) 112 (1999) 531–552.

[45]. Wen Y, Roudebush SL, Buckholtz GA, Goehring TR, Giannoukakis N, Gawalt ES, Meng WS, Coassembly of amphiphilic peptide EAK16-II with histidinylated analogues and implications for functionalization of beta-sheet fibrils in vivo, Biomaterials 35 (19) (2014) 5196–5205. [PubMed: 24680662]

[46]. Altiok EI, Santiago-Ortiz JL, Svedlund FL, Zbinden A, Jha AK, Bhatnagar D, Loskill P, Jackson WM, Schaffer DV, Healy KE, Multivalent hyaluronic acid bioconjugates improve sFlt-1 activity in vitro, Biomaterials 93 (2016) 95–105. [PubMed: 27086270]

[47]. Zbinden A, Browne S, Altiok EI, Svedlund FL, Jackson WM, Healy KE, Multivalent conjugates of basic fibroblast growth factor enhance in vitro proliferation and migration of endothelial cells, Biomater. Sci. 6 (5) (2018) 1076–1083. [PubMed: 29595848]

[48]. Lam J, Segura T, The modulation of MSC integrin expression by RGD presentation, Biomaterials 34 (16) (2013) 3938–3947. [PubMed: 23465825]

[49]. Litvinov SV, Balzar M, Winter MJ, Bakker HA, Briaire-de Bruijn IH, Prins F, Fleuren J, Warnaar SO, Epithelial cell adhesion molecule (Ep-CAM) modulates cell-cell interactions mediated by classic cadherins, J. Cell Biol. 139 (5) (1997) 1337–1348. [PubMed: 9382878]

Statement of significance

The unique concept of the work centers on the genetic fusion of an Fc-binding domain and a self-assembling domain into a single polypeptide. To our knowledge, such bi-functional peptide has not been reported in the literature. The impact of the work lies in the ability to display IgG antibodies and Fc-fusion proteins of any specificity. The data shown demonstrate the platform can be used to localize IgG *in vivo*, and can be tailored for controlling deposition of primary thymic epithelial cells (TECs). The results support a biomaterials-based strategy by which TECs can be delivered as functional units to support T-lymphocyte development *in vivo*. The platform described in the study may serve as an important tool for immune engineering.

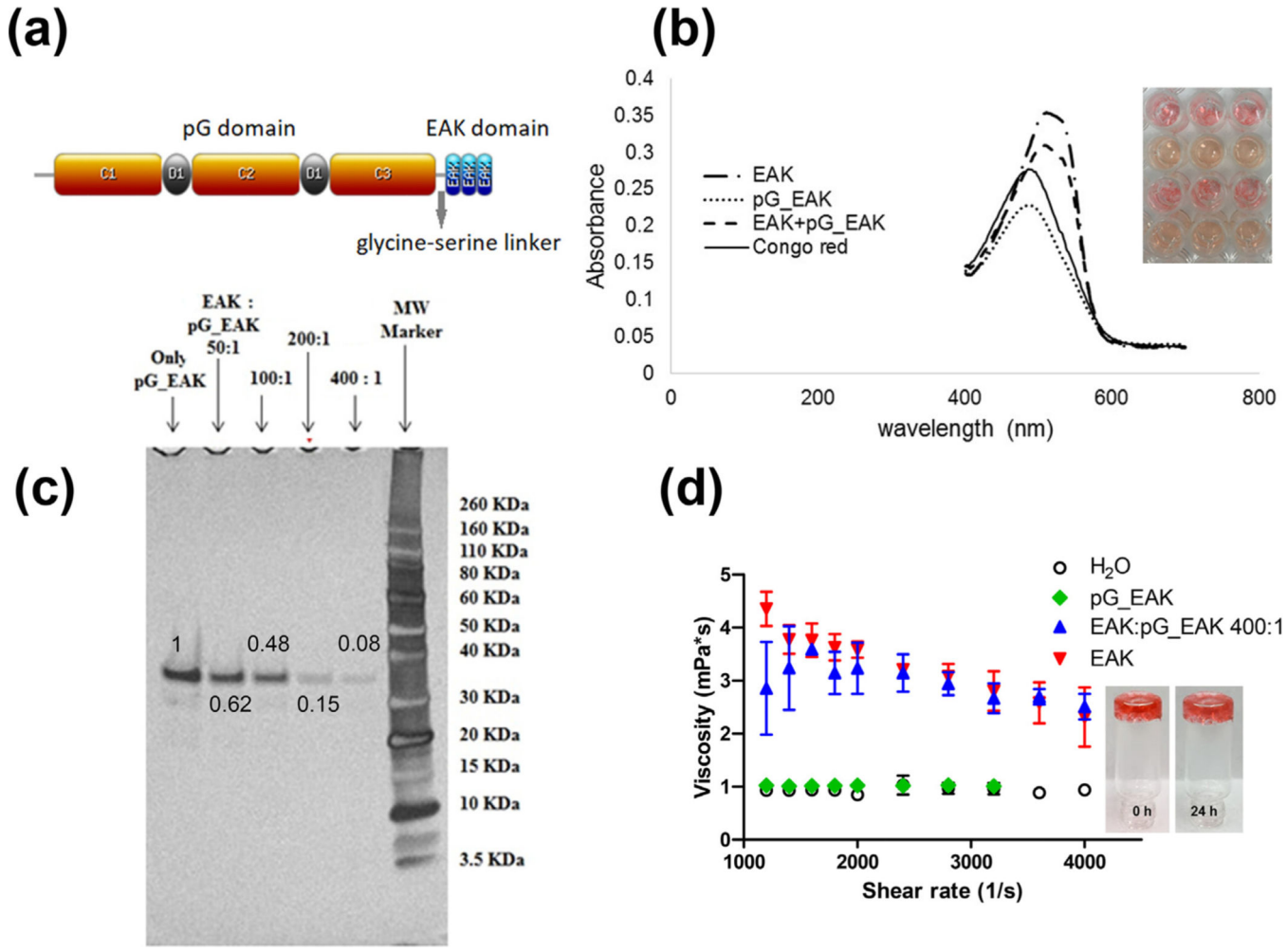

Fig. 1.

Sequence of the Fc-binding SAP fusion peptide pG_EAK. (a) The polypeptide is consisting of three Fc-binding domains in C1, C2, and C3 separated by D1 and D2 sequences and amphiphilic EAK repeats; (**b**) Congo red spectra of PBS solutions containing EAK, pG_EAK, a mixture of EAK and pG_EAK, and solution containing only the dye, showing peak intensities at 510 nm, 486 nm, and 506 nm, and 485 nm, respectively; (**c**) SDS-PAGE electrophoresis of unincorporated fraction of pG_EAK in the mixing; the fractions were quantified using ImageJ profile plot as indicated on the band with mixing ratio at 50:1, 100:1, 200:1, and 400:1 for EAK to pG_EAK; the numbers indicate the fraction of pG_EAK not incorporated into the fibrils; (**d**) viscosity profiles of solutions of PBS containing only EAK (1.5 mg/ml; red downward triangle), only pG_EAK (2.3 μM; green diamond), and EAK intermixed with pG_EAK (400:1; blue upward triangle) using μVISC (Rheosense). (For interpretation of the references to color in this figure legend, the reader is referred to the web version of this article.)

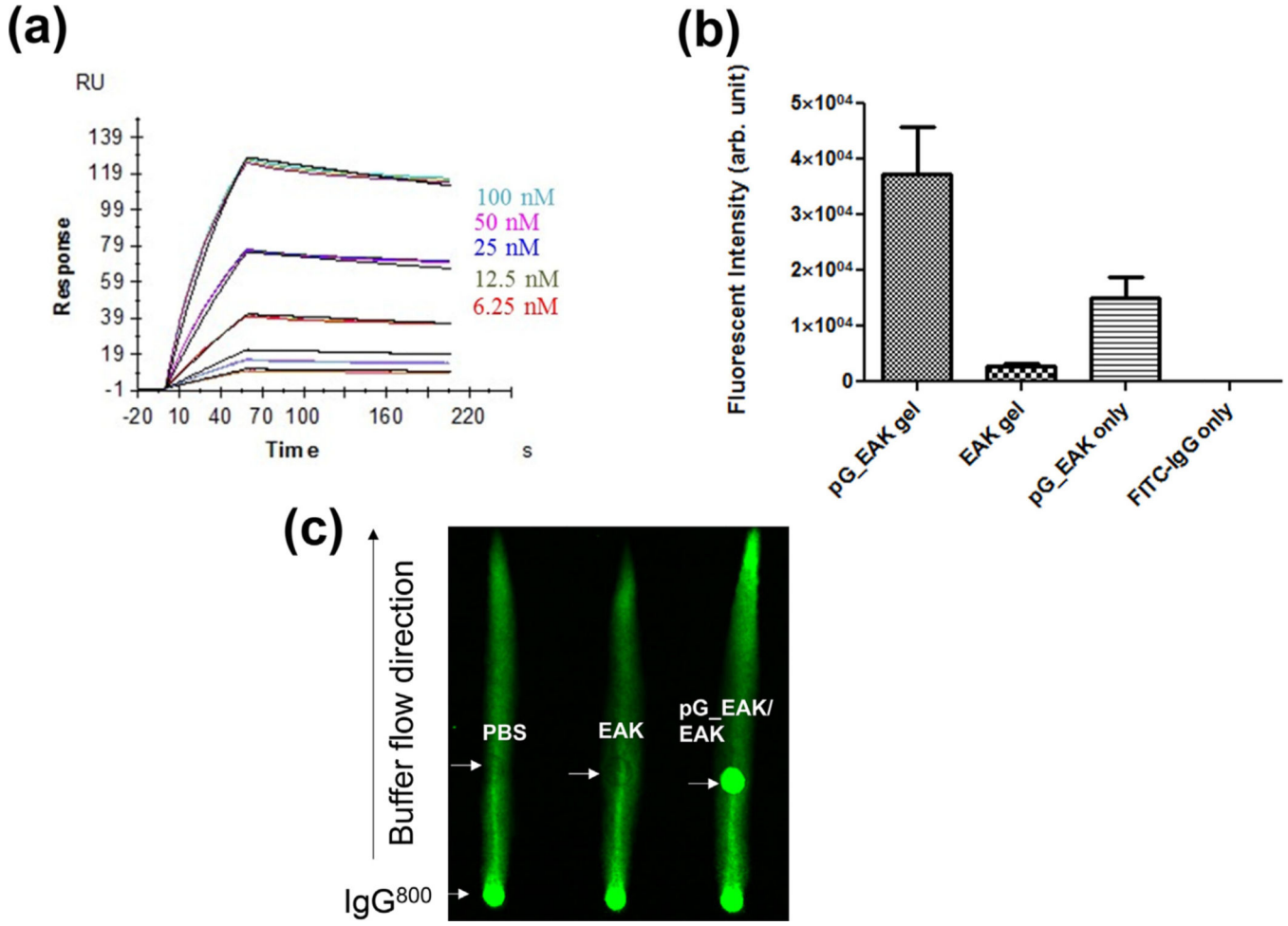

Fig. 2.

Capture of IgG on pG_EAK *in vitro*. (**a**) SPR sensorgrams of pG_EAK ("ligand") interactions with human polyclonal antibodies ("analyte"); the colored lines indicate different concentrations of the IgG tested; Each cluster shows the steady state interaction of the antibody with the modified chip done in triplicate. Saturation of pG binding sites occurred by injecting 100 nM of the antibody; reversal of analyte and ligand, and antibodies of other species yielded similar constants (Table 2); (**b**) Co-precipitation of IgGFITC with buffers containing pG_EAK and EAK ("pG_EAK/EAK gel"), EAK ("EAK gel"), pG_EAK only, and without either peptide ("FITC-IgG only"; n = 3; one-way ANOVA with post-hoc pairwise comparison showing $p < 0.05$ between all pairs); centrifugation of IgGFITC alone (without EAK or pG_EAK) did not result in detectable aggregates, showing that the fluorescent aggregates induced by pG_EAK/EAK was not an artifact of non-specific aggregation of the antibody; (**c**) capture of IgG by pG_EAK in non-equilibrium flow using Whatman paper imaged using an Odyssey Imager. The left lane one was spot with saline (0.5 μL) 6 cm above the solvent reservoir, the middle was spot with EAK (0.5 μL of 5 mg/ml), and the right lane was spot with pG_EAK (0.5 μL of 2 mg/ml)/EAK gel.

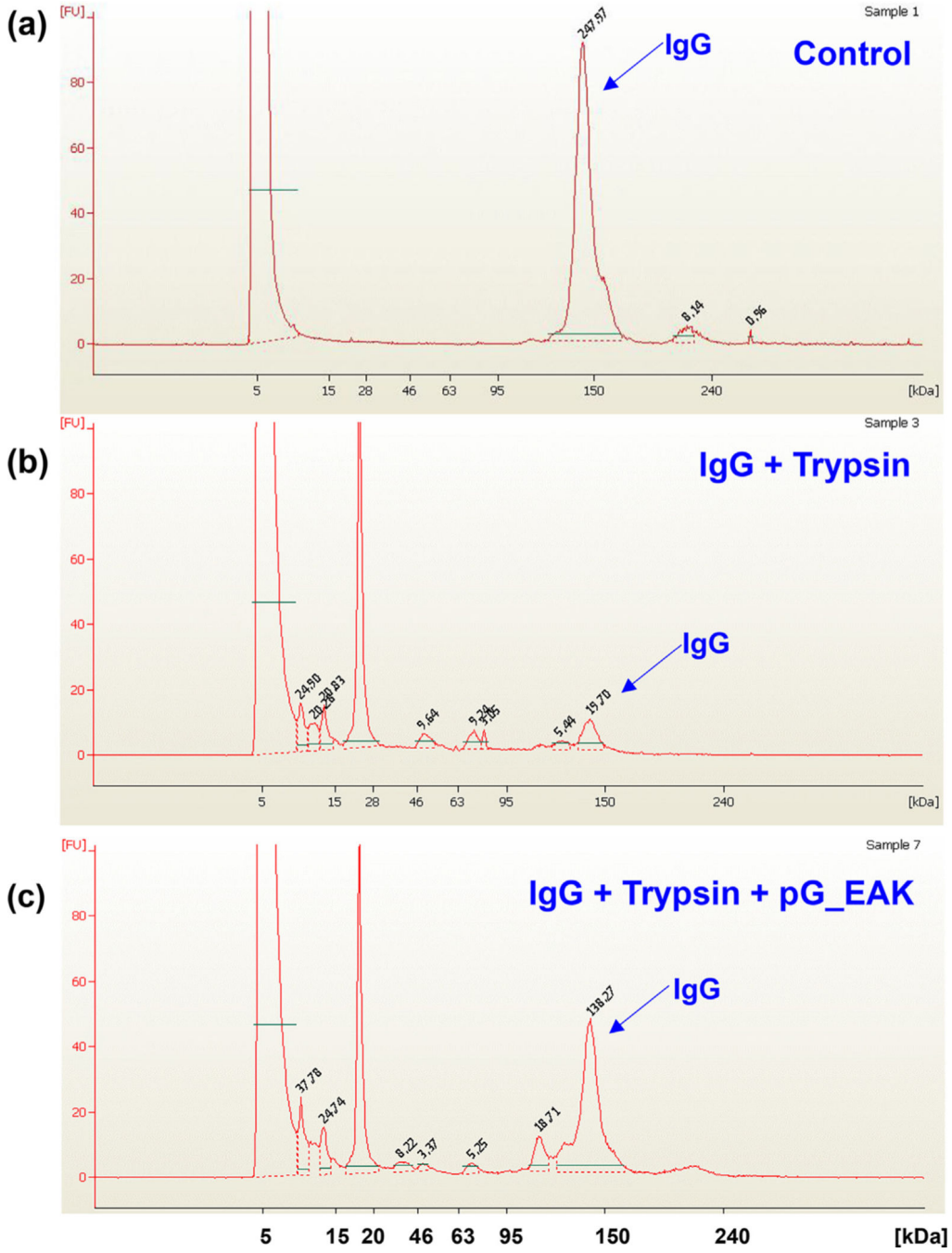

Fig. 3.

Trypsin digestion of human polyclonal IgG following one hour incubation at **37 °C.** (**a**) hIgG alone (**b**) hIgG with trypsin (**c**) hIgG with trypsin and pG_EAK. The supernatants of the mixtures were analyzed using the Agilent High-Sensitivity Protein Chip 250 under non-reducing condition. Results are shown in electropherogram with molecular mass in kDa on the X-axis and concentration-dependent fluorescence on the Y-axis. Intact hIgG creates a peak at the 150 kDa mark, peaks below 150 kDa indicate the presence of antibody fragments from enzymatic degradation. Each peak is labeled with its respective AUC. The y-axis

indicates arbitrary fluorescence unit and all panels are set to the same scale to allow relative comparison.

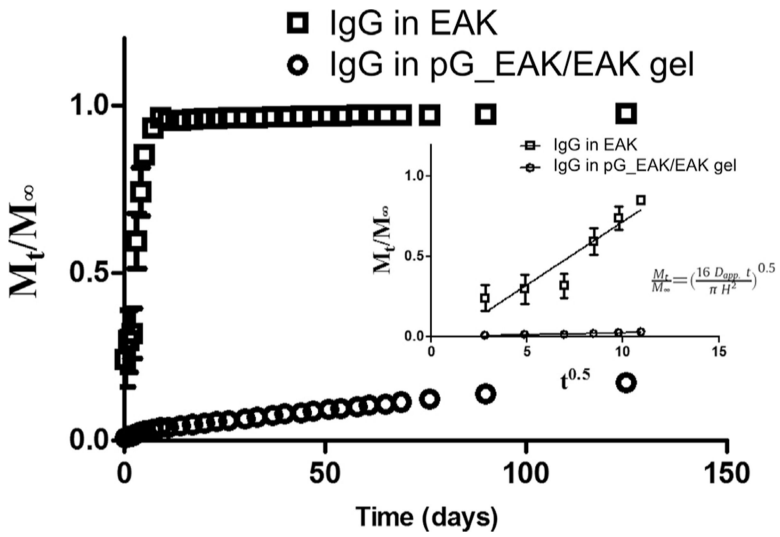

Fig. 4.

Modeling release kinetics of IgG from pG_EAK/EAK gel *in vitro*. (**a**) release profile of IgGFITC embedded in pG_EAK/EAK gel (open circle) and EAK gel (open square) were determined experimentally using a silica vessel of 4.15 mm diameter of the bottom; (**b**) estimation of apparent diffusion coefficients (*Dapp*) based on the first six time points (n = 3), with the assumptions that the gels do not swell; IgGFITC was shown to remain stable for the duration of the experiment, and that the fluorescent intensity correlated linearly with concentration.

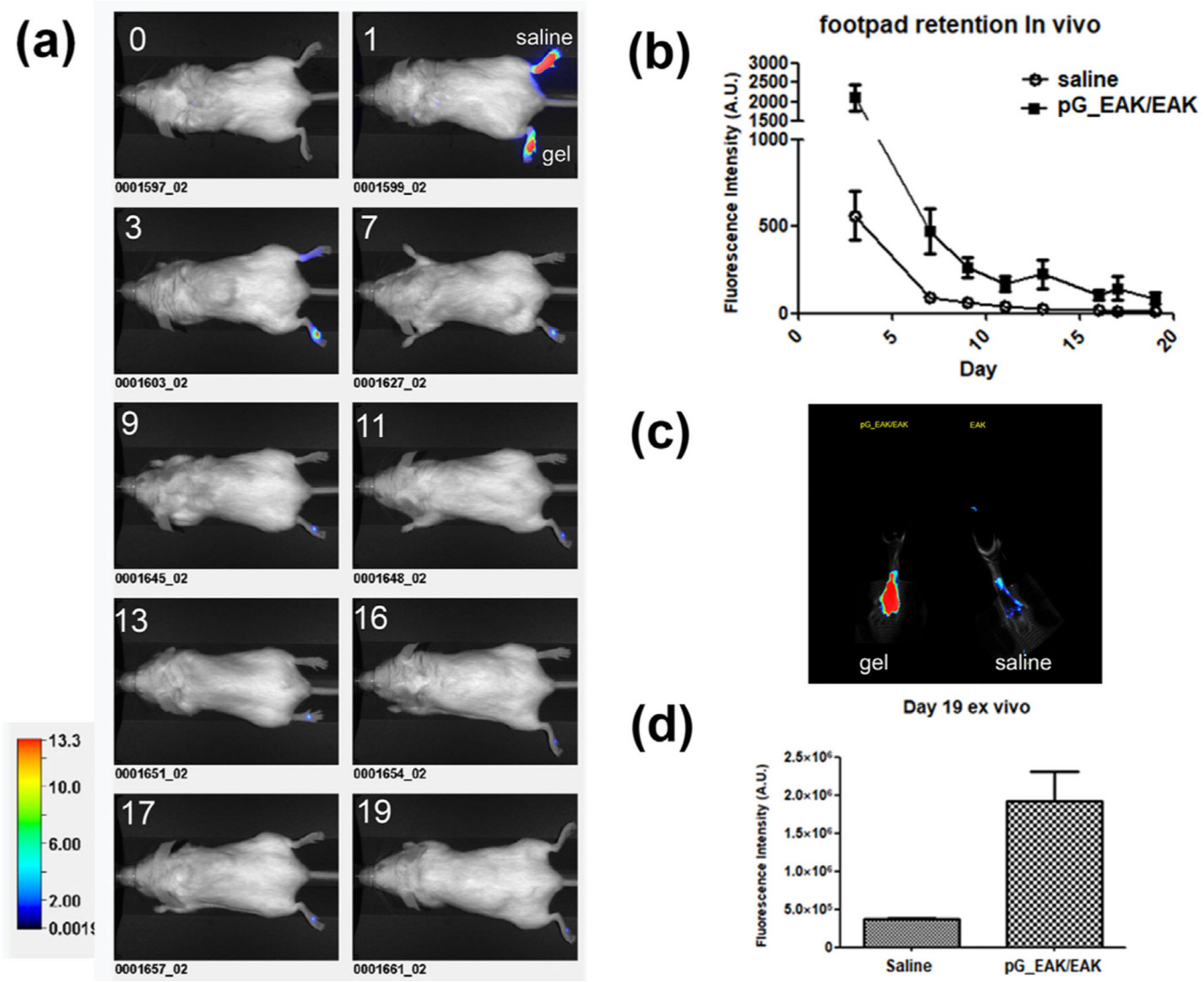

Fig. 5.

In vivo retention of IgG in subcutaneous tissues. IgG800 formulated in saline or in pG_EAK/EAK gel were injected and the signal of the antibody was tracked for 19 days. (**a**) time-lapse images of saline (upper footpad) and pG_EAK/EAK gel (lower footpad) injections captured using Li-Cor Pearl on before injection (“0′′) and immediately after injection (“1”), followed by images on day 3, 7, 9, 11, 13, 16, 17 and 19 as labeled in each panel; (**b**) quantification of the images from day 3 to day 19 ($n = 3$ and $p < 0.05$ on all days during the period, based on Wilcox matched pairs test; (**c**) footpads excised from a mouse were scanned exvivo using a Odyssey imager set at resolution 169 μm and focus offset of 3.2 mm. (**d**) Quantification of the ex vivo images was performed by drawing an region-of-interest around the footpad using a non-fluorescent region as background ($n = 3$; $p < 0.05$, unpaired t-test).

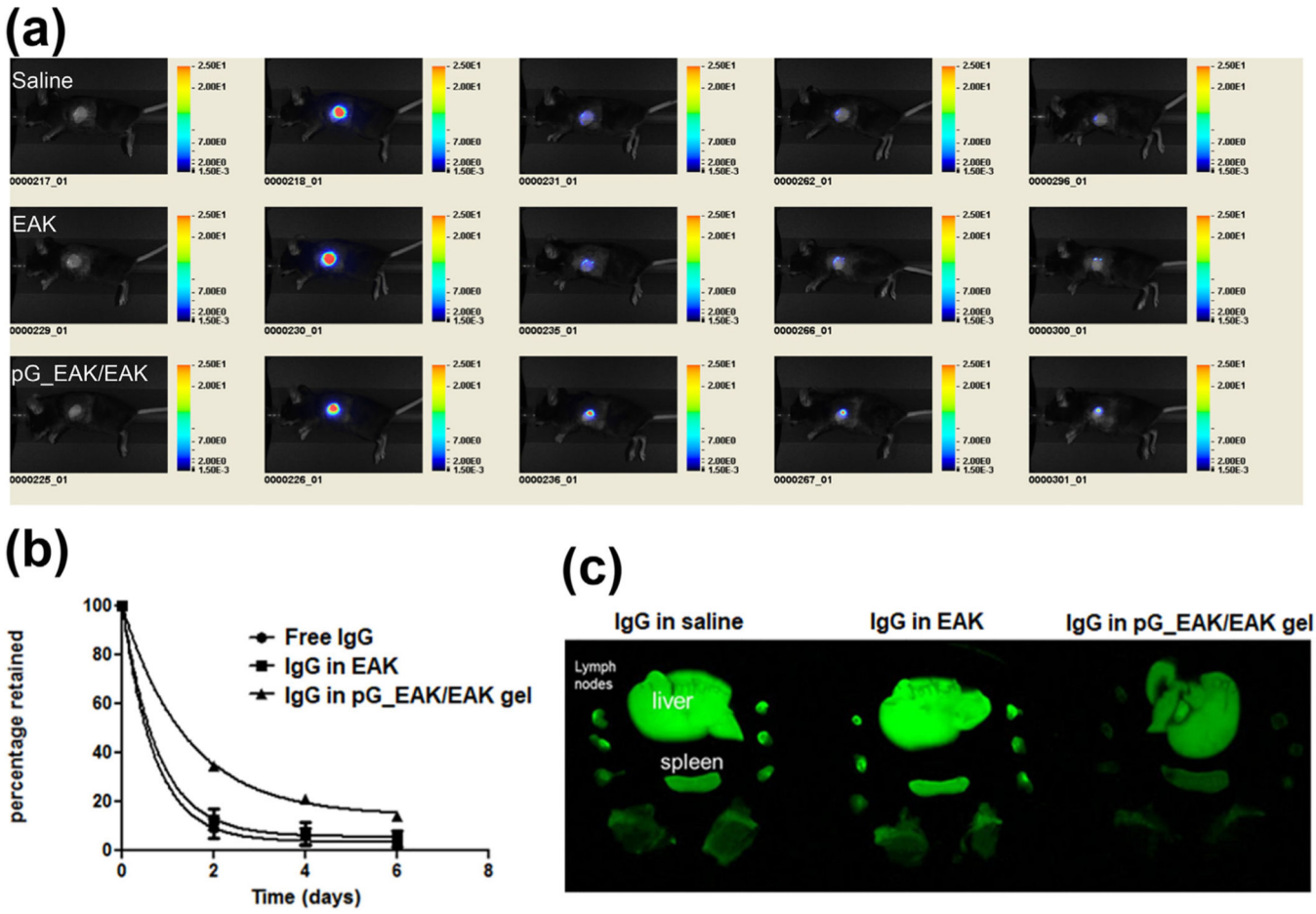

Fig. 6.

In vivo retention of IgG in skin allografts. (**a**) Tracking of IgG800 pre-mixed with saline ("Saline", top row), EAK gel ("EAK", middle row) or pG_EAK/EAK gel ("pG_EAK/EAK", bottom row) injected into skin allografts; each group was done in triplicate, with the figure showing only representative of each treatment. All images were captured in live mice under anesthetization using a Pearl Impulse set the same color scale as shown; pG_EAK used was subjected to an endotoxin removal step; (**b**) data fit to first-order IgG signal decay; the AUC0–6d calculated for free IgG, IgG in EAK and IgG in pG_EAK/EAK gel are 131.6, 144.8 and 229.1, respectively. (**c**) Distribution of the antibody in liver, draining and non-draining lymphoid nodes, and spleen, excised 6 days after injection. Images were captured shortly after excision.

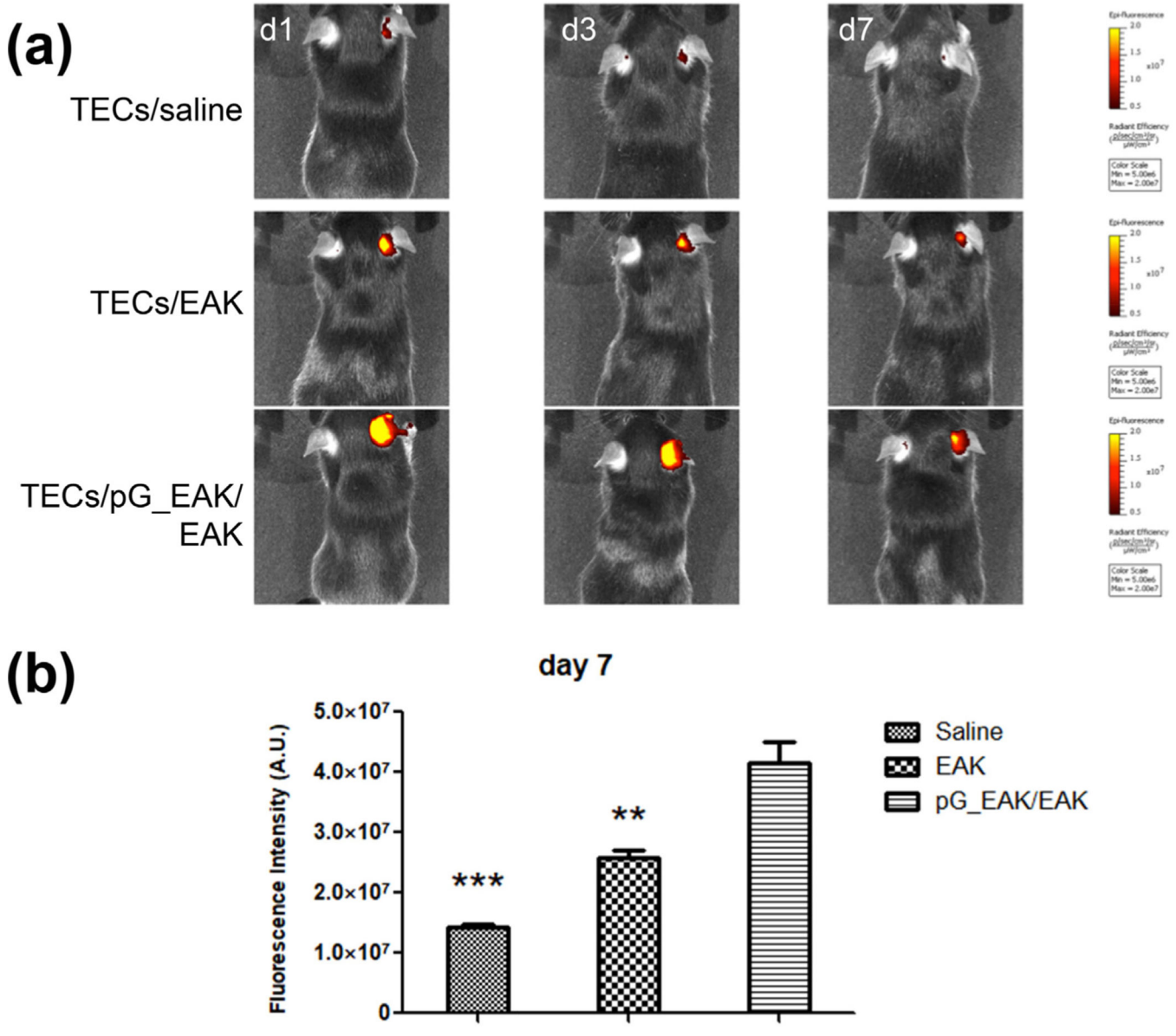

Fig. 7.

Engraftment of TEC/pG_EAK/EAK thymus organoids in the pinna region of outer ears. TECs were harvested from C57BL/6J mice, stained with Qtracker 800, admixed with anti-EpCAM IgG loaded pG_EAK/EAK hydrogel, injected subcutaneously in the right outer ears of syngeneic B6 mice (n = 3). Qtracker 800 stained TECs without gel or loaded in EAK gel were injected to the same location of different mice as the control (n = 3). The presence of Qtracker 800 on mice were imaged on day 1, 3 and 7 using IVIS live animal imager. (**a**) one mouse in each cohort of mice injected with TECs formulated in saline, EAK, or pG_EAK/EAK gel imaged set at the same color scale are shown; (**b**) quantification of retention on day 7 (n = 3; one-way ANOVA; Tukey's multiple comparison test of TECs/pG_EAK/EAK vs TECs/saline, ***$p < 0.001$, and TECs/EAK **$p < 0.01$).

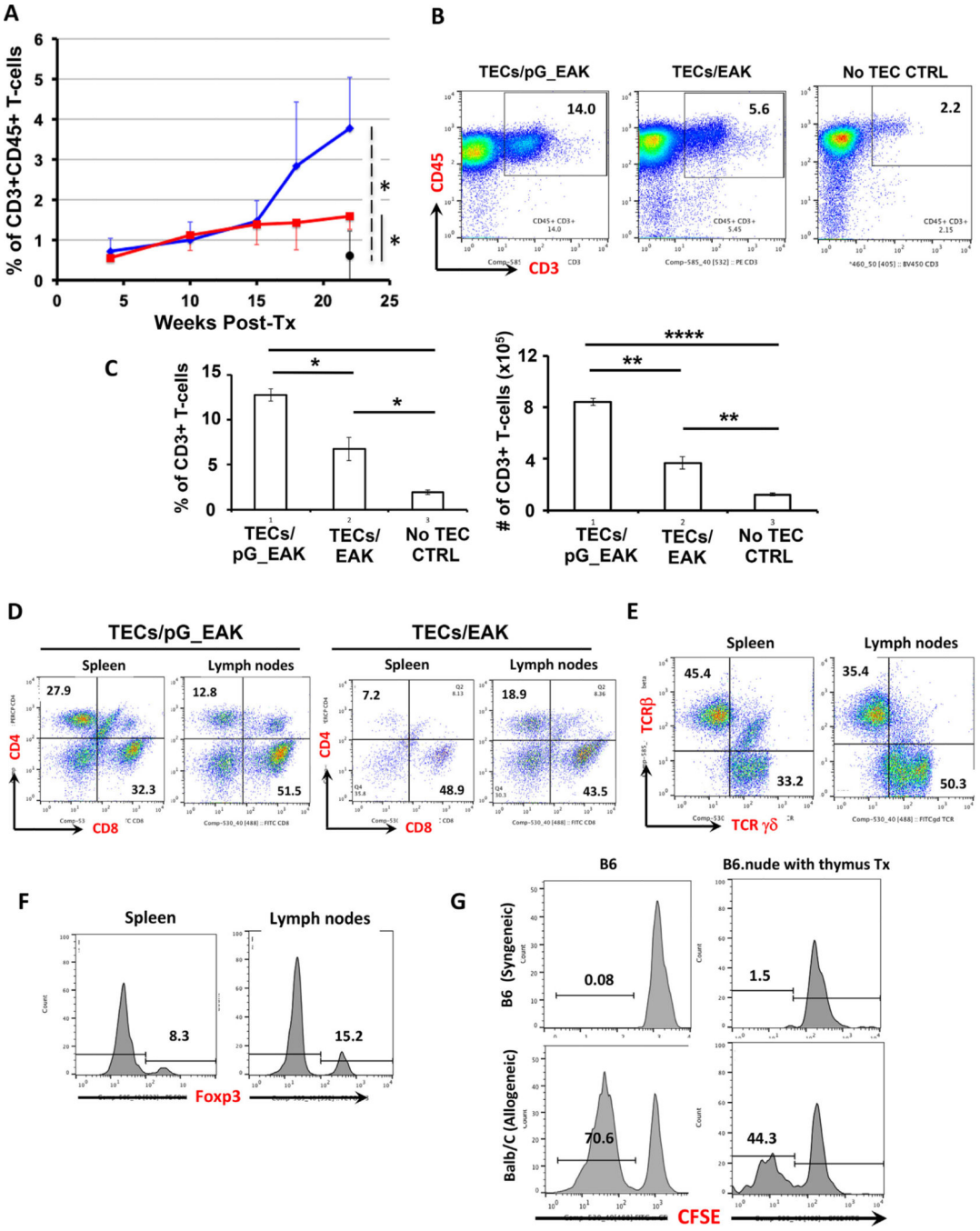

Fig. 8.

Development of functional T cells in athymic B6.nude mice engrafted with TECs pG_EAK/EAK thymus organoids. B6.nude mice were subcutaneously injected with thymus organoids constructed with B6.TECs and pG_EAK/EAK hydrogel in pinna of outer ears. (**a**) Development of CD3+ CD45+ T-cells in blood circulation of B6.nude mice engrafted with B6.TECs/pG_EAK/EAK thymus organoids (TECs/pG_EAK mice, blue line, n = 4), or B6.TECs/EAK control thymus organoids (TECs/EAK mice, red line, n = 3). The black closed circle show the % of CD3+ CD45+ cells in untreated nude mice of similar age

(No TEC CTRL, n = 4). (**b-c**) Axillary, brachial, and inguinal lymph nodes were harvested from the TECs/pG_EAK mice (n = 3), the TECs/EAK mice (n = 3) and the No TEC CTRL mice (n = 3) at 32–36 weeks post injection, and analyzed with flow cytometry. Representative FCM profiles are shown in b, with the numbers inside the boxes representing the percentages of CD3+ CD45+ T cells. The percentages (*left panel*) and the numbers (*right panel*) of the CD3+ T cell populations are shown in **c.** Data are presented as mean ± SEM. * $p < 0.05$, ** $p < 0.01$, *** $p < 0.001$, **** $p < 0.0001$. (**d-f**) Development of CD4+ and CD8+ TCRαβ T cells (d), γδT cells (e) and T regulatory cells. (f) and in spleens and lymph nodes of TECs/pG_EAK mice. Shown are representative FCM profiles (n = 3), with the numbers inside each quadrant representing the percentage of cells in gated population. (**g**) Representative FCM histograms showing the proliferating responses of Tcells isolated from the thymus engrafted B6.nude mice when exposed to allogeneic antigens (Balb/C, lower panels), in comparison to those of T-cells isolated from age-matched wildtype B6 mice (n = 3). Numbers represent the percentages of proliferating T cells in the MLR. (For interpretation of the references to color in this figure legend, the reader is referred to the web version of this article.)

Table 1

Formulations used in back, under-graft, and footpad injections.

	Test[a]		EAK Control[b]		Saline Control[c]	
	Normal	**Graft**	**Normal**	**Graft**	**Normal**	**graft**
EAK	800 μg	200 μg	n.d.	200 μg	n/a	n/a
pG_EAK	30.4 μg	7.6 μg	n.d.	n/a	n/a	n/a
IgG	45 μg	11.2 μg	n.d.	11.2 μg	45 μg	11.2 μg
Volume[d]	207.4 μL	36.7 μL	n.d.	36.7 μL	207.4 μL	36.7 μL

nd: not done

n/a: not applicable

[a]"System" formulation used in experiments shown in Figs. 5 and 6.

[b]"Control" formulation used in experiments shown in Fig. 6.

[c]"Control" formulation used in experiments shown in Figs. 5 and 6.

[d]Injection volume

Table 2

Binding and kinetic constants of pG_EAK polypeptide determined using SPR[#]

	K_D (nM)	k_{on} (1/Ms)	k_{off} (1/s)
Mouse monoclonal IgG	23.1	9.44×10^5	21.81×10^{-3}
Goat polyclonal IgG	0.005	3.66×10^5	2.0×10^{-6}
Rabbit polyclonal IgG	8.0[≠]	1.38×10^5	11.06×10^{-4}
Human polyclonal IgG	7.0[≠]	1.27×10^5	8.93×10^{-4}
Mouse Fc fusion protein	609[≠]	3.93×10^3	23.95×10^{-4}

[#]pG_EAK was immobilized as the “ligand” with the antibodies as “analytes” with dissociation time at 600 s for mouse and goat IgG, and 150 s for rabbit, human and mouse Fc fusion protein

[≠]The reversed setup (antibodies as ligands and pG_EAK as analyte) was performed yielded K_D 13.8 nM, 1.1 nM, and 33.8 nM (150 s dissociation) for rabbit, human, and mouse Fc IgG, respectively.